DROP SIZE DISTRIBUTION IN SPRAYS BY IMAGE PROCESSING

E. Fantini**, L. Tognotti* and A. Tonazzini**

* Dipartimento di Ingegneria Chimica
Università degli Studi di Pisa
Via Diotisalvi, 2
I-56100 Pisa
Italy

** Istituto di Elaborazione della Informazione
Consiglio Nazionale delle Ricerche
Via S.Maria, 46
I-56100 Pisa
Italy

ABSTRACT

An automatic analysis system has been developed and used to analyze photographs obtained by high-speed microphotography, the final aim being to derive the size distributions of drops in sprays.

The problem of determining whether photographic images of particles are in focus or not is solved by obtaining a calibration of geometric parameters of particle images as functions both of the particle position in the camera's field of view and of the particle diameter. On the basis of the results of this calibration on the particular photographic system being used, the drops are automatically rejected or sized and counted.

This is done through a procedure based on the geometrical characterization of drop images at different ranges of gray levels. The main body of such a procedure is constituted by an algorithm of original design (Connected Components Detection Algorithm) which allows for the simultaneous detection of the boundaries of drop images at different gray levels and generates a hierarchical structure among them.

Size distributions obtained by means of the procedure described in the paper offer significant reduction in experimental time as well as improvement in experimental accuracy, in relation to manual sizing and counting techniques.

INTRODUCTION

Photography coupled with image processing is a powerful tool in two-phase flow diagnostics. In a parallel paper (Azzarelli et al., 1988) the advantages of photographic techniques in two-phase flow investigations, as well as the suitability of image processing in spray diagnostics, have both been pointed out.

On the other hand, if measurement of the mean size of the disperse phase (drops, bubbles, particles) is required, visual sizing and counting methods are very tedious, time consuming and suffer from a bias imposed by the operator who usually has to use subjective judgement in placing individual particles into size groups. Furthermore, spray photographs are characterized by the simultaneous presence of drop images with a wide range of "sharpness" of focus. This is not the case of bubbles (Schrodt and Saunders, 1981) and emulsions (Hazlett et al., 1985; Kemel et al., 1987) for which automated and/or interactive image analysis procedures have been developed and applied. Thus for the frequently used semi-automated analysis techniques, the need for the operator to choose "in-focus" drop images in photographs, on the basis of his own opinion, is likely to be a serious source of error.

As a matter of fact, the drop image is sharpest for drops lying in the plane which is focused on the photographic plate of the optical system. As this plane is infinitely thin, it is not possible to measure size distributions by counting only those drops which lie exactly in this plane. As a drop is moved away from this plane the sharpness of its image decreases, thus producing an increasingly thick blurred "halo" around it. It is clear that the selection of the in-focus drops only must be done on the basis of the thickness of this halo, making thus any analysis procedure which relies on the operator's judgement extremely critical. This, together with the dependence of the image characteristics on a number of physical

parameters, gives rise to the need for objective criteria and automatic procedures for the selection of the in-focus drops. But, conversely, it is precisely this problem which represents the main difficulty in the design of a fully automated procedure of drop sizing and counting, as will be seen later.

The objective in the development described in this paper has been to improve accuracy, reduce processing time and maximize the degree of automation in the analysis of spray photographs by using an image analysis system. The procedure described below is almost completely automated and can be applied to solid or liquid particles suspended in any clear gas or liquid. The authors' primary interest has been in the measurement of droplet sizes in liquid fuel sprays produced by twin-fluid atomizers. The capability to measure a wide range of particle diameters, from 10 to 500 μm, with a wide variability of optical properties, ranging from water to heavy fuel oil or coal-water slurries (Andreussi et al., 1988), is required.

AUTOMATED ANALYSIS OF SPRAY PHOTOGRAPHS: PROBLEMS AND PRINCIPLES OF THE PROCEDURE

As mentioned in the previous Section, the simultaneous presence of drop images with a wide range of sharpness of focus can be a serious source of error in a semi-automated procedure of drop sizing and counting, and the main problem in the design of a fully-automated procedure.

Good quality photographs are defined as those in which the images of in-focus drops are sharp, the background density and, as far as in-focus drops are concerned, the density in the center of the images too, are as far as possible uniform, and that overlapping images are at a minimum. Photographic quality is therefore dependent on a number of factors. Among them, is image blur arising from the movements of the drop during the

illuminating flash, the type of film and development procedure used, as well as optical factors related to the camera lens, magnification and spray density.

Moreover the changes in the characteristics of the photographic image of a drop, as it becomes out-of-focus when it moves away from the plane of best focus of the camera, is also a function of drop position, drop size, drop optical properties, and the characteristics of the light source. These complex relations result in a large drop appearing, subjectively, to be in-focus while a small particle in the same transverse plane appears to be out-of-focus.

The derivation of a theoretical description of the dependence of image characteristics on these various parameters is difficult, thus an experimental calibration procedure is necessary to achieve a greater accuracy than could be obtained by purely theoretical treatments.

Figure 1 represents qualitatively typical intensity profiles for both an in-focus and an out-of-focus drop.

Ideally an optimum in-focus drop should display a flat profile on the top but this is not the case in practice because of resolution limitations. From the intensity profiles, it can be seen that the gradients at the edges of the drops reflect the degree of focus of the drops and can be used as the criteria by which drops are chosen for measurements (Ramshaw, 1968; Yule et al., 1978; Jones and Serjeant, 1979). Two intensity levels, I_2 and I_3, which define a "halo" around the drop, can be identified. If level I_2 is set such that it yields the actual diameter of the drop, say d, I_3 can then be used to determine a halo whose width will be called $\Delta d/2$. This can be used for the rejection of out-of-focus drops and the correction of their size, on the basis of a calibration exercise. Thus the intensity levels I_2 and I_3 will be fixed proportions of the intensity

difference between the level I_4 of the background and the level I_1 of the center of the drop image.

A frequent problem is constituted by the presence - in the image - of overlapping drops, ligaments and sheets formed during the breakup processes, as well as agglomerates of poorly focused drops which form non-circular images. These can be distinguished by a shape test: for each drop, detected for example at level I_2, the shape factor perimeter^2/area can be computed. If the drop is not circular this factor is significantly greater than 4π and the drop is rejected.

The considerations made above about the image characteristics of drops that are either out-of-focus or non-circular provide objective criteria for their rejection. Nevertheless, as already pointed out, to perform such a rejection through a fully-automated system of image analysis is not an easy task, the main difficulty being the requested ability, for such a system, to detect the blurred outer region (halo) of the drop and measure it in relation to the size of the inner region (core).

This problem often has been seen to be unsolved in existing literature. In fact many proposed systems have only "black/white" detection, i.e. they can treat binary images only (Sato et al., 1977; Toner et al., 1978). But even when the system can perform the detection of drops at different gray levels, the problem still remain of correctly associating each halo with the corresponding core. For instance, in Ow and Crane (1980), this is done by the intervention of the operator with the use of light pens or other commercial analyzers.

In this paper we propose a solution to this problem based on the detection of the halo and core boundaries of the drops and their hierarchical organization according to a relation of inclusion among curves. This is done by means of an original algorithm (Connected Component Detection Algorithm) which, more in

general, performs the detection and the labelling of connected components in a gray level image (Fantini, 1988).

The C.C.D. Algorithm is part of a set of modules designed for the sizing and counting of the drops and which refers to the objective criteria defined by means of the above mentioned calibration exercise. This set of modules has been integrated in a hardware-software system for general purpose image processing, in order to have a stand-alone system for the processing of digital images from spray photographs. The modular organization of such a system allows for the arrangement of various procedures for the management and analysis of spray pictures. In particular, a special procedure (Drop Size Distribution Procedure) has been designed and organized that, starting from a set of photographs of a spray, enables the drop size distribution of the spray itself to be evaluated.

IMAGE PROCESSING SYSTEM

In the following we will give a short description of the main features of the general purpose image processing system herein referred to. We make reference to the parallel paper by Azzarelli et al. (1988) for a more detailed description of its characteristics and organization, and of its utilization in various tasks of image processing and analysis.

The hardware part of the system itself is composed of:

1. a microphotometer (MFA/36/LS) which digitizes the analogic image, in the form of a 35 mm negative; the resulting digital image, of size up to 1024x1024 pixels, quantized on up to 256 gray levels, has a spatial resolution of up to 12 μm/pixel;

2. a Central Processor Unit, which processes the digital image (memory 1MB, clock 12 MHz, MS-DOS);

3. a mass memory, constituted by a high density floppy disk and a 40 MB hard disk;

4. a pictorial card connected to a RGB monitor for the displaying of the processed image.

The software part of the analysis system can be divided in three main environments (Azzarelli et al., 1988):

1. the processing environment in which the modules and the procedures of acquisition, pre-processing, geometric transformations, photometric corrections, noise reduction and general purpose analysis (mathematic or logic operation, segmentation, classification, etc.) are contained;

2. the utility environment which contains modules and routines for the general purpose management of images;

3. the thematic processing environment which contains special modules designed for solving problems related to particular applications.

DROP SIZE DISTRIBUTION PROCEDURE

As already pointed out, through the integration between suitable modules contained in the above described image processing system and the thematic modules for drop sizing and counting, a special procedure has been designed and organized that enables the drop size distribution in a spray to be evaluated, from a set of photographs of the spray itself.

To facilitate comprehension, it is convenient to operate a subdivision of the whole procedure into five consequential logic phases, identified as acquisition, pre-processing, drop detection, drop discrimination and drop counting (Fig.2).

The acquisition, carried out by means of the line scanner MFA/36/LS, transforms the image into a mxn matrix of 256 gray levels. In this phase the operator chooses the resolution of acquisition and, if necessary, the zones in the image to be digitized. However, once the resolution has been fixed, the whole image can be digitized automatically and sequentially. The digitized image, residing in the frame memory of the pictorial card and displayed on the TV monitor, can be stored and labelled, and the minimum and maximum intensity levels I_m, I_M are also provided.

The next step is the pre-processing, which the operator can decide to use or not, on the basis of the quality of the image. In dense or wide sprays, the background and the maximum intensity levels can be similar, with the result of the reduction in contrast of the image. Furthermore, fuel spray images recorded from a high temperature, high pressure chamber, have low frequency intensity degradation. This is due to droplets that hit the observation window and to refracting gradients in the optical path. Procedures may be used which allow for reduction of the noise as well as contrast enhancement (Azzarelli et al., 1988). Oberdier (1984) and Bertollini et al. (1985) also reported methods of shading correction on images from the pulsed laser illumination of fuel sprays.

The drop detection phase is performed by means of a Connected Component Detection Algorithm that constitutes by far the most original part of the whole procedure. This algorithm will be described in detail in the next Section, due to its general applicability to a wide range of problems in Image Analysis and Recognition. In the following, a description will be given of the principles upon which it is based and of its specific application to the problem at hand.

Let us consider the image under investigation as constituted by light droplets on a dark background. If the gray levels of the image occupy the range $[I_m,I_M]$ of the grayscale, it is then possible to define two threshold levels, say I_2 and I_3, such that the three ranges $[I_m,I_2)$, $[I_2,I_3)$ and $[I_3,I_M]$ identify the gray levels of the background, and the halos and cores of the drops respectively (Fig.1). In such a way the image can be considered to be virtually equivalent, without the loss of information, to a 3-level image, and the background, the halos and the cores can be described by the connected clusters of pixels, all having the same gray level (connected components).

Fig.3a shows a 3-level synthetic image which illustrates some typical drop arrangements frequently observed in a spray photograph. Black, gray and white represent the background, halos and cores, respectively.

Clearly, a vector description of the external boundaries of the connected components, together with their hierarchical organization based on a relation of inclusion among curves, will describe the contents of the image completely, i.e. identify and discriminate the drops and their halos.

These vector descriptions, in terms of x-y coordinates in the image plane, and the related hierarchical structure, are retained as necessary and sufficient information for the successive drop discrimination and drop counting phases, performed through the geometrical characterization of the drop boundaries.

The boundaries detected in the image in Fig.3a are shown in Fig.3b as an example of the drop detection phase.

As regards the intensity levels I_2 and I_3, they are a function of the intensity difference between the background I_4 and the center of the drop image I_1, on the basis of the calibration procedure described in the following. The major operator function is simply to define I_1 and I_4 by interactive analysis of the image. It is important to note that the background is generally taken to

be greater than the minimum value I_m, on the basis of the image histogram, as the mean value of the background; whilst level I_1 coincides generally with the maximum value I_M. It means that I_1 is defined as the level at the center of the largest in-focus drop in the image (and it involves a slight underestimation of the true diameter of the smaller drops) and it must be taken into account during the calibration.

The drop discrimination phase consists in the rejection of all the out-of-focus and/or non-circular drops that are not to be considered in the evaluation of a significant drop size distribution inside the spray. In this phase the thickness $\Delta d/2$ of the halo is evaluated as half the difference between the diameters of the external boundaries of the halo and the core respectively. Analogously, the shape factor perimeter^2/area will be evaluated on the basis of the boundary of the core. Then the drop is rejected if the thickness of its halo is greater than a certain function $H^*(d)$ of the actual diameter d of the drop, or if the shape factor differs more than a certain ε from 4π. $H^*(d)$ and ε are obtained by means of the calibration exercise. The relation of inclusion among halos and cores produced by the Connected Component Detection Algorithm provides a further rejection criterion, based on the presence of more than one core inside the same halo. Fig.3c shows the drops left after the drop discrimination phase, with reference to the image in Fig.3a.

At the end of the discrimination phase, only the in-focus circular drops that have passed the above described tests will be retained and analyzed by the last phase of the procedure, in order to produce different size distribution and statistic momenta of the diameter of the drops. In this phase the measured diameter d_{MEAS} is corrected by means of the correction algorithm yielded by the calibration procedure, which, obviously, depends on the optical system and the spray on study.

The drop counting phase is applied to a large number, say M, of in-focus circular drops, detected by analyzing a sufficient number of images.

Let us consider to subdivide the range $[d_{min}, d_{max}]$ of the diameters of the drops into N classes of equal width given by

$$\Delta d = \frac{d_{max} - d_{min}}{N} \qquad (1)$$

and call m_k the number of particles whose diameter falls inside the k-th class, i.e. has a value in the range $[d_{min}+k\Delta d, d_{min}+(k+1)\Delta d)$, with k=0,...N-1. Of course it will be

$$\sum_{k=0}^{N-1} m_k = M \qquad (2)$$

In accordance to the previous definitions, the statistical moment $d_{p,q}$ of the order p-q will be given by the value

$$\bar{d}_{p,q} = \left(\frac{\sum_{k=0}^{N-1} m_k \bar{d}_k^p}{\sum_{k=0}^{N-1} m_k \bar{d}_k^q} \right)^{\frac{1}{p-q}} \qquad (3)$$

where d_k is meant to be the mean diameter inside the k-th class.

Analogously, the distribution of the order p will be given by the sequence

$$P_p(\bar{d}_k) = \frac{m_k \bar{d}_k^p}{\sum_{k=0}^{N-1} m_k \bar{d}_k^p} \qquad k=0, 1, ..., N-1 \qquad (4)$$

An example of the application of the above described procedure to the real image of a spray will be illustrated further on.

CONNECTED COMPONENT DETECTION ALGORITHM

The problem of detecting drops in a photographic image of sprays, as formulated in the previous Sections, can be seen as a particular case of the more general problem of describing a digital image, quantized on L distinct gray levels, by the set of connected clusters of pixels all having the same gray level (connected components). Such a description is particularly meaningful when each connected component can be related to precise features of the image, such as objects or parts of objects contained in it, and represents a fundamental tool in pattern analysis and recognition tasks.

The most typical example is given by binary images constituted by "dark" objects on a "light" background or viceversa. In this case the "dark" connected components represent the information of interest in the image. Several algorithms have been proposed (Cunningham, 1981) for detecting connected components in binary images, and most of them produce a vector description of their boundaries, which can be used for geometrical analysis and characterization of the corresponding objects.

Nevertheless, often, two gray levels alone are not sufficient to adequately describe the contents of an image, as in the cases in which the detection of particular structures or details inside the

objects is required. That is the case of the problem at hand in which at least three gray levels are needed to represent the image of a spray without the loss of information: a level for the background, a level for the halos and a level for the cores of the drops.

In these cases the detection of connected components is much more complicated than in the case of binary images, due to the fact that they must be qualified on the basis of their own color, and a relationship among them must be pointed out.

In Fig.4a, the problem is illustrated through a synthetic image. Different patterns evidence different colors, and the numbers indicate the various connected components to be detected. In Fig.4b the hierarchical structure among the connected components is reported by using a tree-like representation.

The algorithm here proposed (Fantini, 1988) solves the problem of detecting connected components at assigned values or ranges of gray level values in images quantized on any number of gray levels. Once the set of gray levels of interest has been defined, all the pixels having other gray levels will be considered to logically belong to the background, itself treated as a connected component.

For each connected component its external boundary is detected, and an entry in a list of descriptors is formed that enables a complete characterization of the connected component itself, with the consequent possibility to distinguish it among the others. In particular, in this list different descriptors are related by references that determine a hierarchical structure among connected components, based on a relation of inclusion, and for each of them there is a pointer that addresses a circular list containing the x-y coordinates of the relative external boundary.

More in detail, each entry in the list of descriptors is composed of the following fields:

- value of the gray level of the connected component
- pointer to the related circular list that contains the boundary coordinates
- pointer to the connected component identified as parent of the current one (if its value is 0 the parent is the background)
- pointer to the connected component identified as first child of the current one (if its value is 0 there are no children)
- pointer to the connected component identified as first brother of the current one (if its value is 0 there are no brothers)

The structure of the list of descriptors makes it possible to easily locate a given connected component inside the hierarchy, i.e. to know its eventual 'parent', 'children' and 'brothers'. This facilitates the computation of parameters of interest, depending on the particular image analysis problem to be solved. For instance, with reference to Fig.4, it could be useful to compute the total area occupied by the connected components number 1, 2 and 3, or only that of number 1.

For the algorithm to run correctly, all the connected components under investigation must be surrounded by a frame constituted of background pixels. In this way, the background boundary will always be the first boundary detected in the image, creating thus a reference mark for the following relationships among connected components.

The detection of the boundaries is performed by means of a connectivity analysis on pixels having the same color. It is noteworthy to precise that such an analysis is executed at the same time for all the boundaries, by means of a unique image

inspection, realized through a scan-line process from top to bottom and from left to right with reference to the image plane. For each row, all the sequences of pixels of the same color (runs) are found and each one gives rise to a new entry to be added to a list (run-length list) that contains the features of the runs themselves, summarized in the following parameters:

- pointer to the relative connected component in the list of descriptors
- number of the current scan-line
- value of the gray level of the run
- x-coordinate of the first pixel of the run
- x-coordinate of the last pixel of the run

After detecting all the runs in the current scan-line, their connections with the runs of the previous scan-line are investigated.

Runs that have no connections with the runs of the previous scan-line identify a new boundary, thus giving rise to a new entry to be added to the list of descriptors of the connected components.

The process that detects the connections among runs of two adjacent scan-lines also takes into account more complex situations, such as the merging of pseudo-boundaries related to the same connected component, and the closing of a boundary (Fig.5). These situations give rise to an updating of the list of descriptors, and in particular of the pointers that define the hierarchy.

After connections among runs have been identified, the references to the circular list are suitably set in the run-length list. In this way, once a boundary has been closed, it is possible to detect its coordinates automatically.

The generation of the hierarchy proceeds in parallel with the connectivity analysis and at the end of the last scan-line the background boundary will be closed, in such a way as to complete the whole hierarchical structure for all the connected components of the image.

CALIBRATION

Since the changes in the characteristics of the photographic image of a drop as it becomes out-of-focus is a function of many factors, the results of a calibration exercise will depend on the particular apparatus being used, including the light source and type of film. Thus the calibration has been performed for the apparatus usually employed in our spray characterizations. Such an experimental set-up, described in detail in a previous paper (Chella et al., 1986), is constituted by a light source of original design, a 35 mm camera and various optics. A 135 mm lens with 30 cm extension tubes, and a x2 rear converter, yielding a 5.25-folds magnification on the negative plate, have been used in the calibration. The relative aperture was 2.8. The system was used for local characterization of coal-water slurry sprays (Andreussi et al., 1988).

A graticule with 10 circles of precisely known diameters from 30 to 340 μm has been used. Photographs of the graticule at different distances from the best in-focus plane were taken.

Thus the external boundaries at the two levels I_2 and I_3 were determined. The choice of these values is not critical, provided that the same values are used for both calibration experiments and the particle size measurements. The level intensity I_2 was

arbitrarily set such that it individuates the actual circle diameter, for in-focus circles, I_3 to define a halo; so it was obtained:

$$(I_2-I_4) / (I_1-I_4) = 0.25 \qquad (5)$$

and I_3 was arbitrarily fixed as:

$$(I_2-I_3) / (I_1-I_4) = 0.12 \qquad (6)$$

Once the intensity levels I_2 and I_3 had been defined, the behavior of the halo widths and of the measured diameters of the calibration circles was monitored as a function of the position relative to the plane of focus. For the imaging system used, Fig.6 illustrates the halo width variation with position for some of the calibration circles, whereas Fig.7 relates its halo width, h, actual diameter, d, and measured diameter, d_{MEAS}. The data reported in Figs.6 and 7 are related to a 3 mm depth of field. The halo width is non-symmetrical with respect to the plane of best focus, for this particular optical configuration. In all the data, as a particle was moved away from a central position in one of the camera's fields of view, h increased and d_{MEAS} increasingly underestimated the true particle diameter d. It can be noted that the d_{MEAS} vs. h plots for each size can be reasonably fitted by straight lines of the form

$$d_{MEAS} = D(d) - K(d)\, h \qquad (7)$$

where K(d) decreases, in absolute value, as size increases and D(d) increases linearly with increasing d.

Fits to the empirical D and K distributions were obtained and have the form

$$D = A + B\, d \;\; ; \;\; K = C\, d^{-n} \qquad (8)$$

with A=70, B=0.866, C=36.3, n=0.335 and d expressed in microns.

This calibration experiment also shows that particles less than 100 μm could be detected only within a 1 mm depth of field. In other words, the actual depth of field reduces from 3 to less than 1 mm as particle diameter reduces from 340 to 30 μm. This effect is caused by the more rapid variations in image light intensity distribution which occur after a drop or particle has been moved beyond the distance from the best focus plane, at which the uniform light intensity distribution across the center of drop images disappears. Beyond this position the intensity was a Gaussian distribution with a central peak intensity I_c. The value of I_c decreases as the particle position is moved away from the center of the field of view, until I_c is smaller than the measurement level I_2 and the particle image is no longer detected and measured. This phenomenon occurs first for smaller particle diameters. Thus the value of critical halo H*(d) should be fixed in order to detect and count only the particles inside a certain depth of field. In Fig.7 a curve fit to the data at the limits of 1 mm depth of field is also reported, which defines the envelope of all the values of h and d_{MEAS} within the 1 mm depth of field. The curve has the form

$$H^*(d) = E - F \log d \qquad (9)$$

with E = 15.13 and F = 2.83 (for d >10 μm).

Depth of field of about 1 mm has been widely used in previous works since it allows a detailed spatial resolution of the spray, if compared with laser diffraction particle size analyzers (Andreussi et al., 1988).

Finally, from Eq.(7) and empirical fits of Eqs.(8) it is possible to evaluate the correction algorithm which yields the actual drop diameter as a function of d_{MEAS} and h for the system used in the calibration. In general this procedure is necessary, since the

diameter of the smallest drops tends to be underestimated as the drop position moves toward the limits of the depth of field.

RESULTS

Fig.8 shows the digitized image of a typical water spray, obtained by a Y-jet atomizer in a cold chamber. The photograph, in the form of a negative plate, was obtained by means of the above mentioned apparatus. The presence of well focused and out-of-focus drops can be noted, as well as overlapped images of drops and agglomerates of poorly focused images, produced by the drops outside the camera's field of view.

Fig.9 shows the plot of the boundaries, at intensities I_2 and I_3, after the discrimination phase and, finally, Table 1 reports the corrected data on drops in Fig.9. Only the circular drops, with halo less than H*(d) have been counted and sized.

On average, 20-30 drops per photograph were counted within the 1 mm depth of field in this water spray near the center of the spray cone. Measurement of approximately 500 drops was required in order to produce a repeatable histogram of particle sizes. Total analysis time by the system for one photograph, including the time required to digitize the photograph and derive I_2 and I_3 was about 1-2 minutes. Thus, on average, 30 minutes were required to derive a statistical meaningful size distribution for one position in a spray, from 15-20 photographs. If compared with the several hours required by the less accurate manual or semi-automated techniques, this procedure shows to be a good solution for the drop sizing and counting problem.

Fig.10 reports the histogram of the number distribution of drop diameters after the analysis of 15 photographs, taken in the same position in the spray. If compared with a distribution measured from the same pictures by means of the operator

selecting in-focus drops, it was seen that the manual procedure yielded a smaller number of small drops in the spray. This was caused by the visual effect of smaller drops appearing to lose their focus more quickly than larger drops, as also shown by the results of the calibration exercise.

CONCLUSION

Automated image analysis procedures can be successfully employed in spray diagnostics. In particular, photographs of sprays can be accurately analyzed for drop size distributions by using the almost completely automated procedure described in the paper.

An original algorithm (C.C.D.A.) enables the discrimination of drops to be considered in the sizing and counting task, through the detection of the connected components of an image and their organization in a hierarchical structure.

Focus discrimination should be based on the results of a calibration which measures the changes in the characteristics of particle images as functions of particle positions in the camera's field of view and the particle size.

Size distribution obtained in this way offers a significant improvement in both experimental time and accuracy, as compared with manual techniques used to analyze spray photographs.

REFERENCES

Andreussi P., L. Tognotti, G. De Michele and M. Graziadio. *Aereosol Sci. & Tech.*, in press (1988).

Azzarelli L., M. Chimenti, O. Salvetti and L. Tognotti. Image processing application in spray diagnostics. submitted to *Comput. Chem. Engng.* (1988).

Bertollini G. P., L. M. Oberdier and Y. H. Lee *Optical Eng.* **24**, 464-469 (1985).

Chella G., L. Tognotti and S. Zanelli. *Atomisation Spray Techn.* **2**, 187 (1986).

Cunningham R. Segmenting Binary Images. *Robotics Age*, 4-19 (1981).

Fantini E. Automatic recognition of inclusions among connected components in gray level images. *IEI Internal Report*, in press (1988).

Hazlett R.D., R.S.Schechter and J.K.Aggarwal. *Ind. Eng. Chem. Fundam.* **24**, 101-105 (1985).

Jones A.R. and M.Sarjeant. A high speed photographic system for measuring drop sizes and velocities in dense fuel sprays. *Central Electricity Generating Board Note R/M/N1049* (1979).

Kamel A.H., S.A.Akashah, F.A.Leeri and M.A.Fahim. *Comput. Chem. Engng.* **11**, 435-439 (1987).

Oberdier L. M. An instrumentation system to automate the analysis of fuel-spray images using computer vision. in *Liquid Particle Size Measurement Techniques ASTM STP 848*, (Tishkoff J.

M., R. D. Ingebo and J. B. Kennedy, Eds.), American Society of Testing and Materials (1984).

Ow C.S. and R.I.Crane. *Int. J. Heat and Fluid Flow* **2**, 47-53 (1980)

Ow C.S. and R.I.Crane. *Journal of the Institute of Energy* Sept.1981, 119-123 (1981).

Ramshaw C. *J.Inst.Fuel* **41**, 288-292 (1968).

Sato M., K.Shimuzu and T.Sakai. *J.Inst.Fuel* **50**, 19-22 (1977)

Schrodt V.N. and A.M.Saunders. *Comput. Chem. Engng.* **5**, 299-305 (1981).

Toner M.C., M.J.Dix and H.Sawistowski. A television-microprocessor for high-speed image analysis. *J.Phys. E.: Sci. Instrum.* **11**, 960 (1978).

Yule A.J., N.Chigier and N.W.Cox. Measurement of particle sizes in sprays by the automated analysis of spark photographs in *Particle Size Analysis (Paper 22)*, (Groves M.J., Ed.), Heyden, London (1978)

FIGURE CAPTIONS

Fig.1 Drop image intensity profiles.

Fig.2 Diagram of the Spray Photograph Analysis System.

Fig.3 a) Synthetic representation of typical drop arrangements in spray images.
b) Drop boundaries detected in the image of Fig.3a.
c) Drop boundaries after the drop discrimination phase in the image of Fig.3a.

Fig.4 a) Synthetic representation of connected components of an image.
b) Tree-like representation of the hierarchical structure among the connected components.

Fig.5 At the end of the scan-line A, the two distinct boundaries labelled as 1 and 2 are recognized to be part of the same boundary and then merged into one. At the end of scan-line B, the closing of boundary 3 is recognized.

Fig.6 Halo width variation vs. position in field

Fig.7 Relation between measured and actual diameters and halo width.

Fig.8 Digitized image of a water spray.

Fig.9 Plot of the boundaries at I_2 and I_3, after discrimination phase, for drops in Fig.8.

Fig.10 Histogram of number distribution ($d_{V\ 0.5}$ is the volume median diameter).

Table 1 Corrected data on drops in Fig.9.

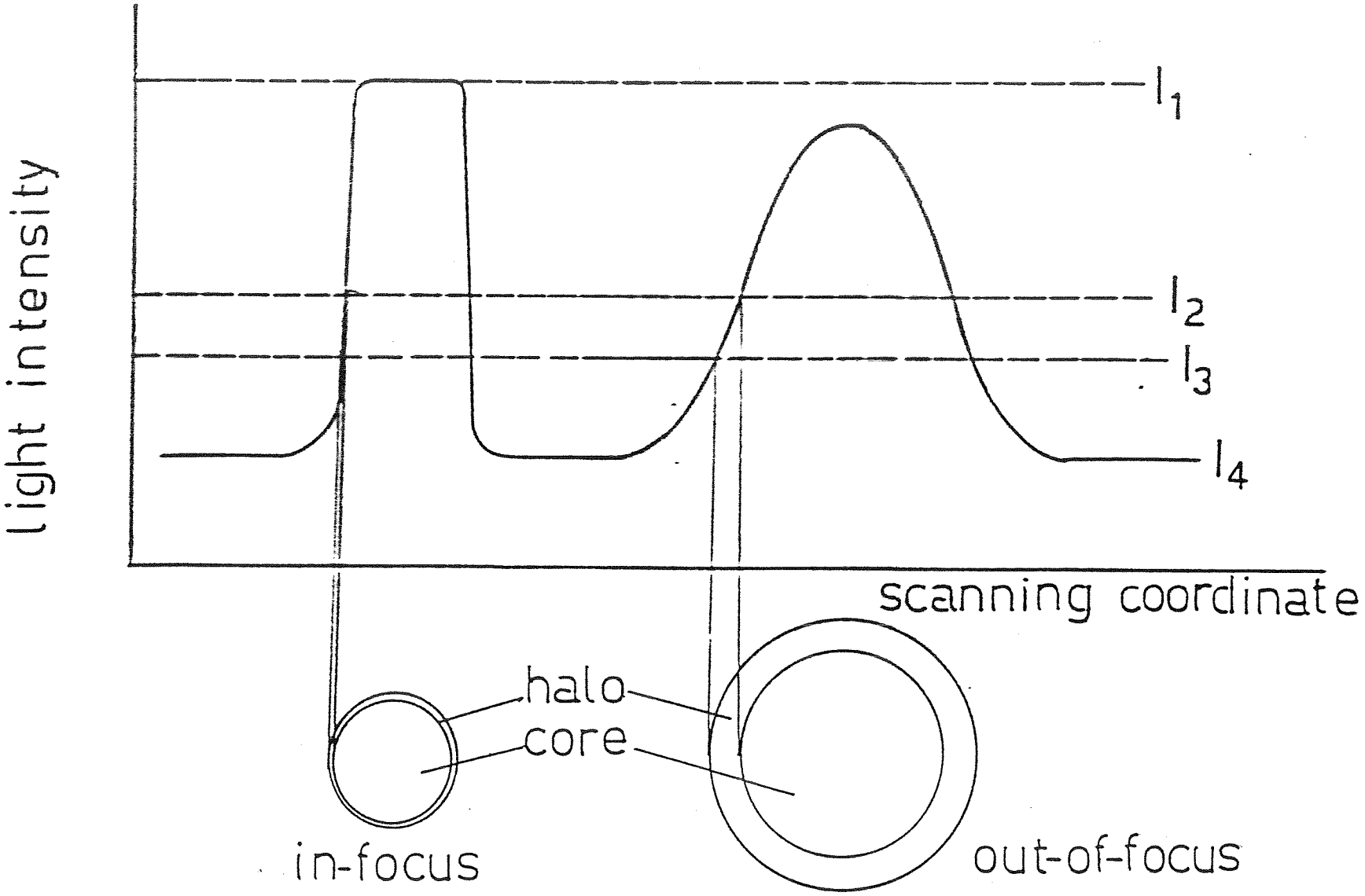
light intensity
I_1
I_2
I_3
I_4
scanning coordinate
halo
core
in-focus
out-of-focus

Fig. 1

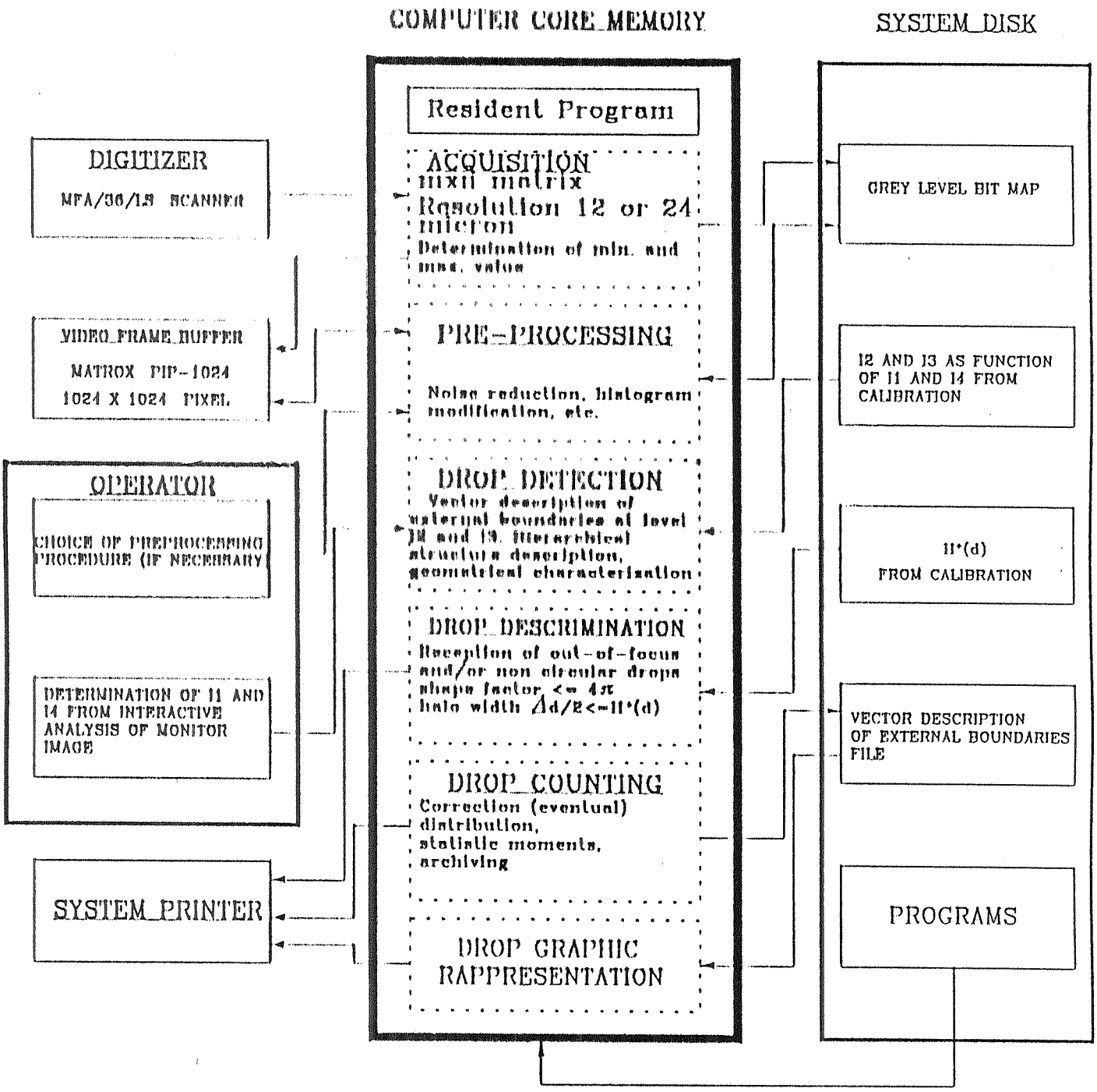
COMPUTER CORE MEMORY
SYSTEM DISK
Resident Program
DIGITIZER
MFA/36/13 SCANNER
ACQUISITION
mxn matrix
Resolution 12 or 24 micron
Determination of min. and max. value
PRE-PROCESSING
Noise reduction, histogram modification, etc.
DROP DETECTION
Vector description of external boundaries of level 11 and 13, hierarchical structure description, geometrical characterization
DROP DESCRIMINATION
Reception of out-of-focus and/or non circular drops
shape factor <= 4π
halo width Δd/2<=11*(d)
DROP COUNTING
Correction (eventual) distribution, statistic moments, archiving
DROP GRAPHIC RAPPRESENTATION
VIDEO FRAME BUFFER
MATROX PIP-1024
1024 X 1024 PIXEL
OPERATOR
CHOICE OF PREPROCESSING PROCEDURE (IF NECESSARY)
DETERMINATION OF I1 AND I4 FROM INTERACTIVE ANALYSIS OF MONITOR IMAGE
SYSTEM PRINTER
GREY LEVEL BIT MAP
I2 AND I3 AS FUNCTION OF I1 AND I4 FROM CALIBRATION
I1*(d)
FROM CALIBRATION
VECTOR DESCRIPTION OF EXTERNAL BOUNDARIES FILE
PROGRAMS

Fig. 2

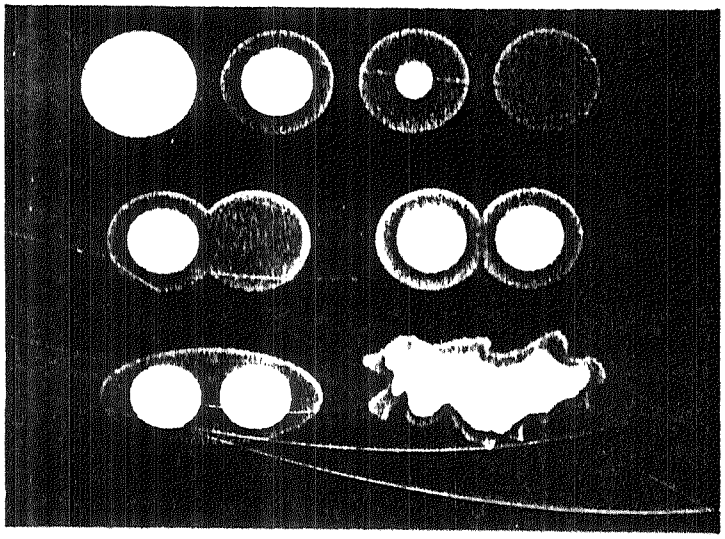

a)

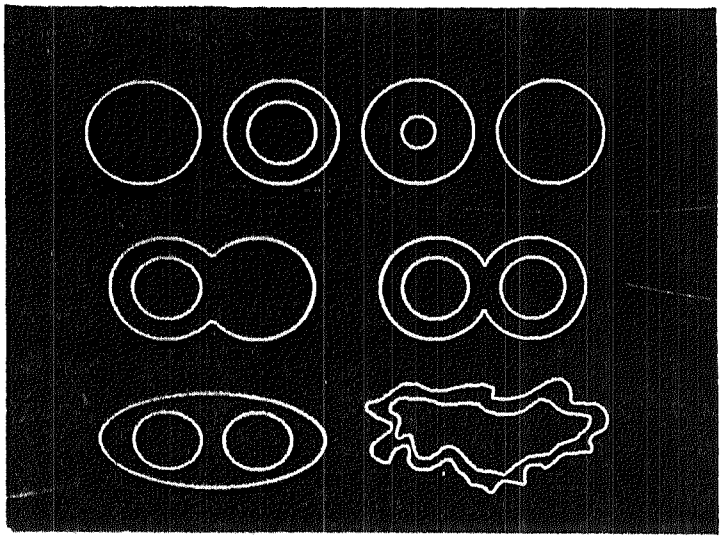

b)

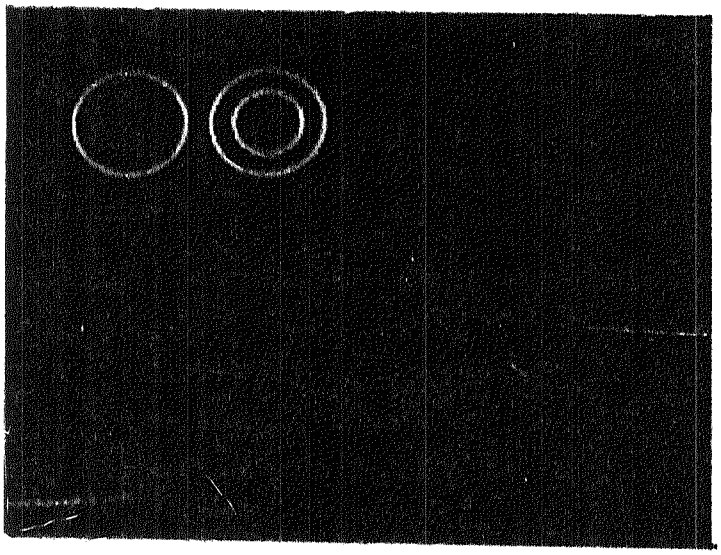

c)

Fig. 3

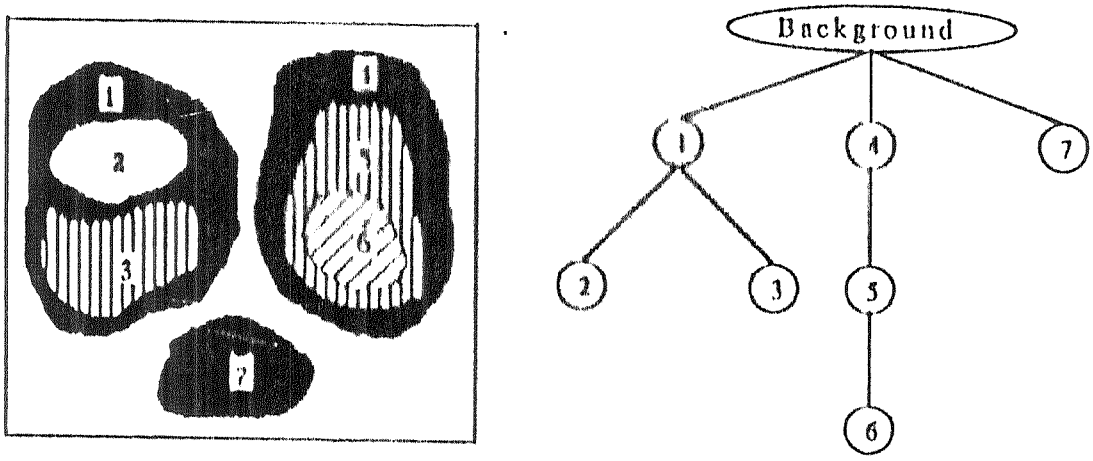

a)

b)

Fig. 4

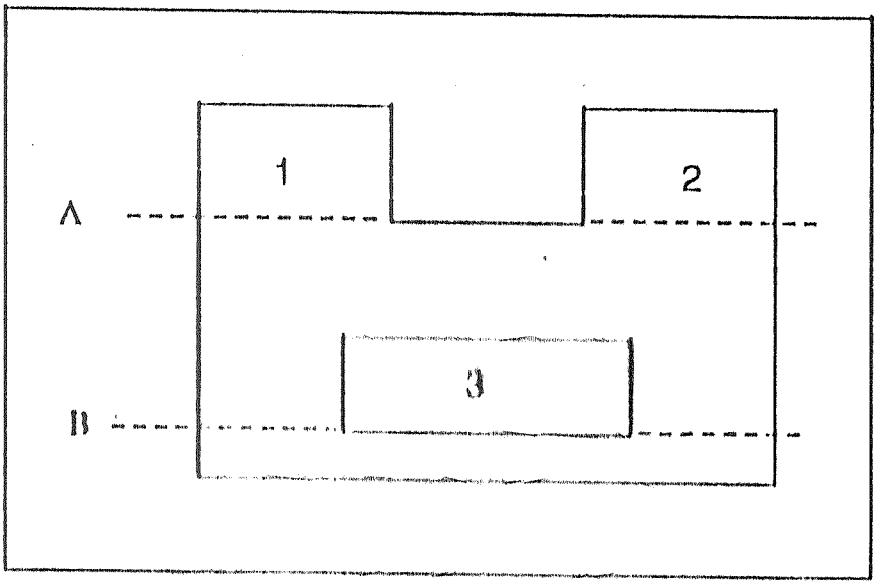

Fig. 5

Fig. 6

Fig. 7

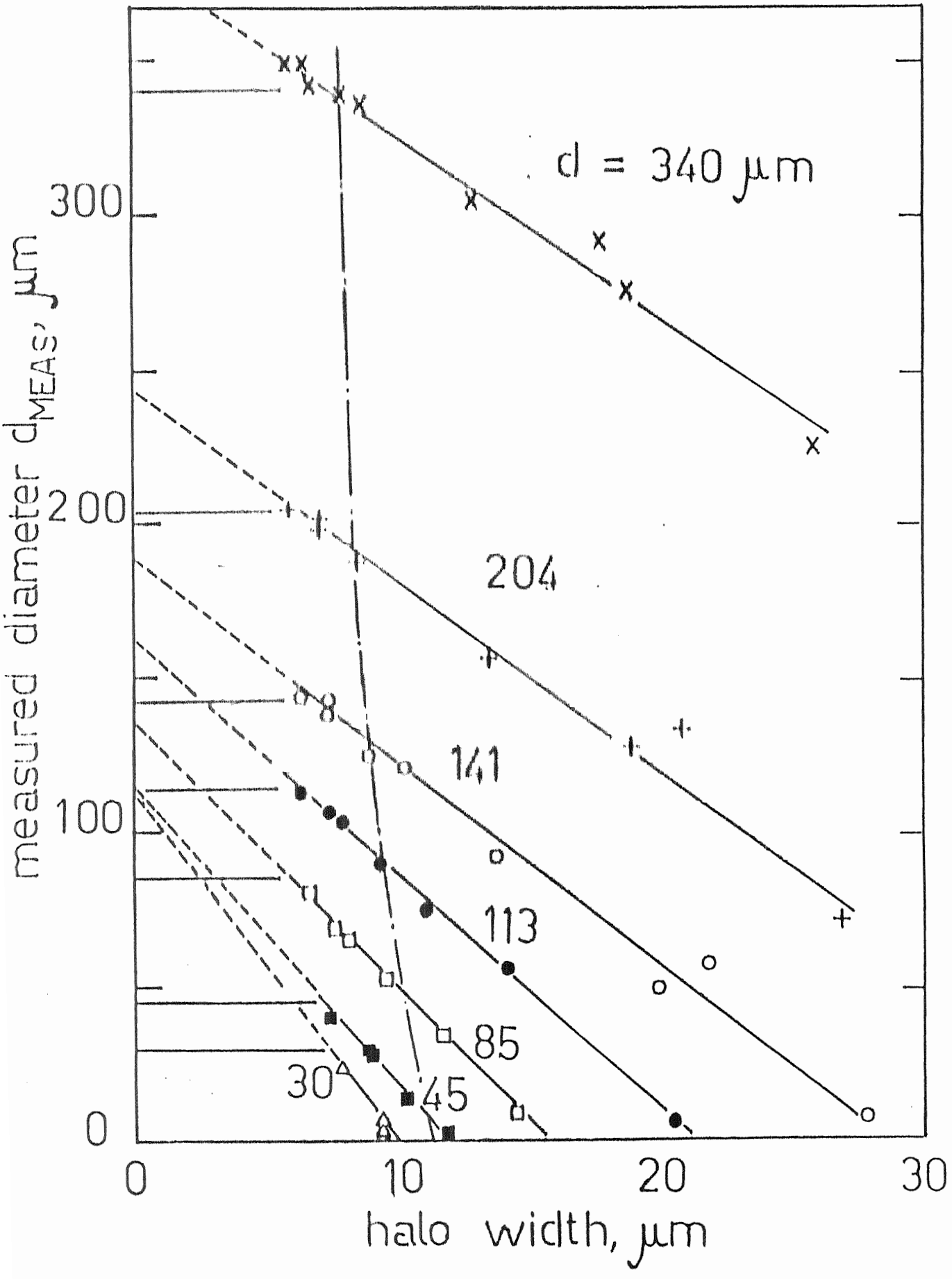
d = 340 µm
204
141
113
85
45
30
300
200
100
0
0
10
20
30
measured diameter d_{MEAS}, µm
halo width, µm

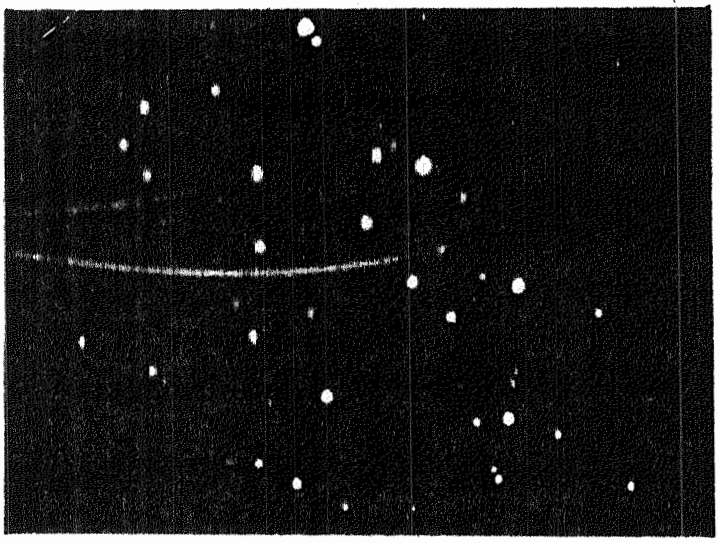

Fig. 8

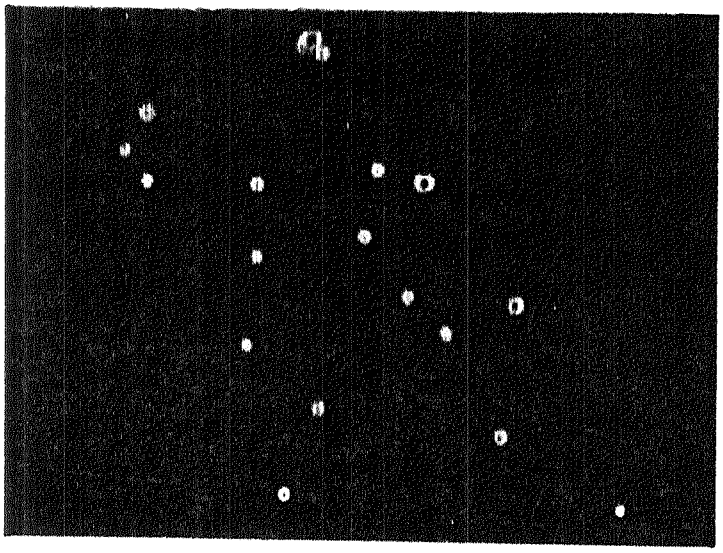

Fig. 9

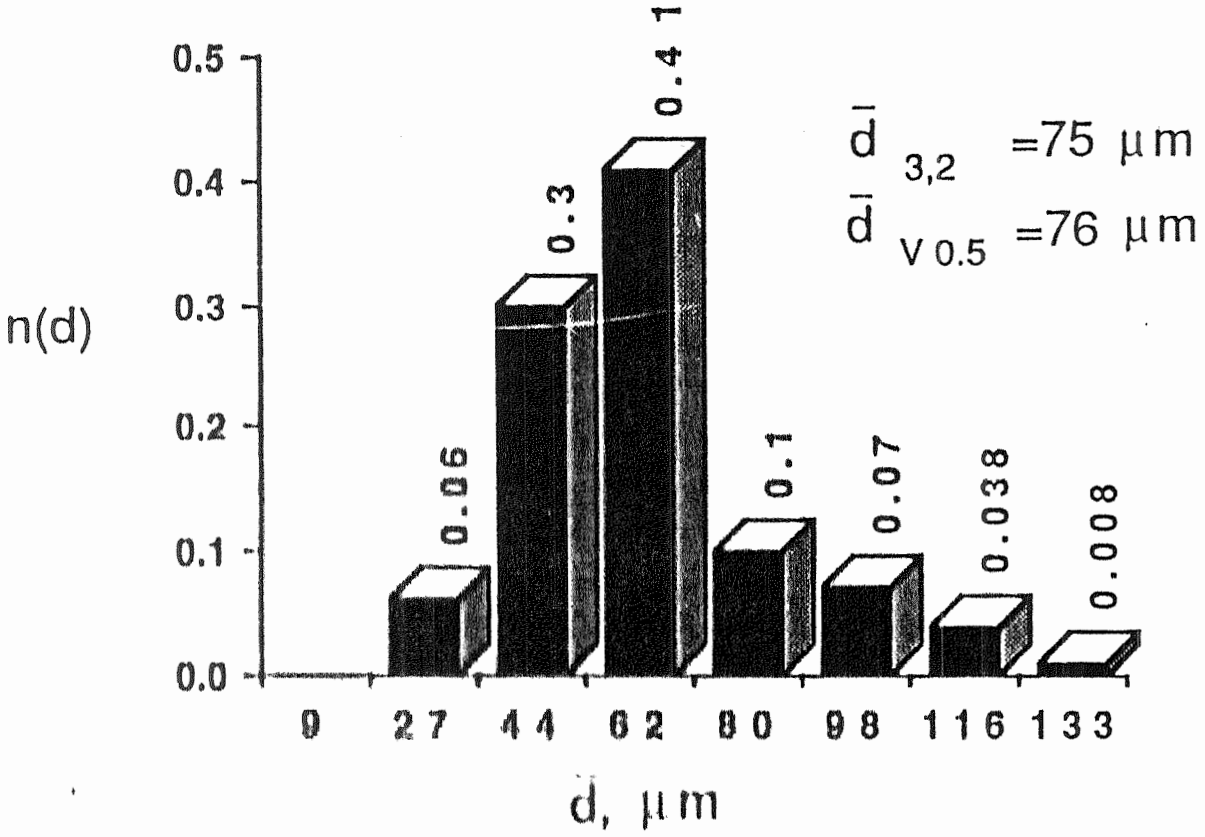
n(d)
0.5
0.4
0.3
0.2
0.1
0.0
0.06
0.3
0.41
0.1
0.07
0.038
0.008
0
27
44
62
80
98
116
133
d, µm
$\bar{d}_{3,2}$ =75 µm
$\bar{d}_{V\,0.5}$ =76 µm

Fig. 10

Area	Perimeter	Diameter	Shape factor
12116.410	406.009	124.206	13.610
2706.237	1060.204	61.351	13.653
31PP.706	1111.074	63.054	15.232
1740.760	154.114	47.117	13.507
2240.406	176.127	53.505	13.797
9035.261	360.239	107.257	14.363
1082.566	124.625	37.126	14.347
2831.326	174.498	60.041	13.361
2240.406	176.247	53.505	13.816
1540.574	145.090	44.219	13.665
P464.777	171.246	58.249	13.725
6479.375	304.258	78.741	13.726
1790.377	151.471	47.745	14.026
777.178	114.411	31.670	15.542
2207.607	178.078	57.191	13.335
4288.626	240.654	73.825	13.504
1740.768	161.127	47.107	14.846
777.292	114.625	35.670	15.542

Table 1